Environmental Engineering and Management Journal *February 2020, Vol. 19, No. 2, 195-204*
http://www.eemj.icpm.tuiasi.ro/; http://www.eemj.eu

"Gheorghe Asachi" Technical University of Iasi, Romania

MACROSPHERICAL POROUS METALLOSILICATE MATERIALS: CHARACTERIZATION AND APPLICATIONS

Emil Ioan Mureșan[1]*, Teodor Malutan[2], Doina Lutic[3], Adrian Puitel[2], Nicanor Cimpoeșu[4], Bogdan Istrate[5]

[1]"Gheorghe Asachi" Technical University of Iasi, "Cristofor Simionescu" Faculty of Chemical Engineering and Environmental Protection, Department of Organic, Biochemical and Food Engineering, 73 Prof. Dimitrie Mangeron Blvd., 700050, Iasi, Romania
[2]"Gheorghe Asachi" Technical University of Iasi, "Cristofor Simionescu" Faculty of Chemical Engineering and Environmental Protection, Department of Natural and Synthetic Polymers, 73 Prof. Dimitrie Mangeron Blvd., 700050, Iaşi, România
[3]"Alexandru Ioan Cuza" University of Iasi, Faculty of Chemistry, Department of Chemistry, 11 Carol I Blvd., 700506, Iasi, Romania
[4]"Gheorghe Asachi" Technical University of Iasi, Faculty of Materials Science and Engineering, Department of Materials Science, 41A Prof. Dimitrie Mangeron Blvd., 700050, Iasi, Romania
[5]"Gheorghe Asachi" Technical University of Iasi, Faculty of Mechanical Engineering, Department of Mechanical Engineering, Mechatronics and Robotics, 61A Prof. Dimitrie Mangeron Blvd., 700050, Iasi, Romania

Abstract

The main goal of this work was to develop a cheap and easy method for the synthesis of the porous metallosilicate macrospheres. Zirconium silicate macrospheres with diameters in the range 1.5 – 1.6 mm were obtained by the spray gelling technique, using the multi templating method. Tetraethyl orthosilicate was used as silica source. The chitosan played a dual role (pore and shape generating agent), while other inexpensive and easily accessible biomaterials including yeast, sugar and gelatin were used as pore generators. The multi templating technique allowed to obtain spherical form particles with large pores which facilitate the access of the reactants to the active centres located inside the pores. The zirconium silicate beads were characterized by nitrogen sorption technique, XRD, FTIR and SEM/EDAX analyses. The synthesized beads were used as adsorbents for the removal of the Astrazon Blue BG dye from aqueous solutions. The adsorption data were analysed through different adsorption isotherm and kinetic models. The dye removal percentage varied from 92.5% to 88.71% when the initial dye concentration varied from 60 mg/L to 150 mg/L (for an adsorbent concentration of 5 g/L and a temperature of 295 K). Due to their size, hardness and shape these materials can be easy handled, recovered and reused.

Key words: adsorption isotherm, adsorption kinetic model, dye, metallosilicate macrosphere, synthesis

Received: January, 2019; Revised final: November, 2019; Accepted: November, 2019; Published in final edited form: February, 2020

1. Introduction

Dyes are important compounds commonly used in various industries such as textiles, printing ink, ceramics, rubber, paper and pulp, leather, cosmetics. Their presence in water even in concentrations less than 1 ppm exert harmful effects on environmental (Hossein and Foroutan, 2019). The dyes can cause allergies, dermatitis, skin irritation, can inhibit the penetration of the sun into the water stream and to disrupt the aquatic ecosystem. Various physical and chemical methods were used for the removal of the dyes from the wastewaters. These include: coagulation/precipitation (Junxing et al., 2018; Rima et al., 2003; Sizykh et al., 2018), microbial degradation (Forgacs et al., 2004; Znoozi et al., 2018),

* Author to whom all correspondence should be addressed: e-mail: eimuresan@yahoo.co.uk, Phone: +40232278683/ 2135; Fax: +40232 271311

chemical oxidation (Cristiana et al., 2009; Nassar et al., 2017) and adsorption (Largitte and Pasquier, 2016; Sohrabnezhad and Pourahmad, 2010). However, the adsorption is the most efficient alternative with a high potential for the removal and the recovery of the dyes from the wastewaters. The most widely used adsorbents include activated carbon (Al-Degs, 2001; Kumar et al., 2017), graphene oxide (Sun et al., 2014; Konicki et al., 2017), lignite (Gurses et al., 2014), mesoporous silica (Chih-Hyng et al., 2011; Peige et al., 2018); zeolites (Briao et al., 2018; Xu et al., 2014); clays (Betega de Paiva, 2008; Huang et al., 2017; Tehrani-Bagha et al., 2011), biowastes (Bellu et al., 2010; Gottipati and Mishra, 2010), ion exchange cellulose monoliths (Yang et al., 2019), polydopamine-modified fibers (Wang et al., 2019). In the last years, the requirement for environmental and more efficient technologies amplified the interest for the use and the development of the hierarchical porous materials (Hammed et al., 2016; Jamwal et al., 2017; Muresan et al., 2015; Rutkowska et al., 2015; Xu et al., 2014).

This type of materials contains at least two types of pores and present the advantages associated with each level of porosity, from selectivity to mass transfer: high surface area (due to the presence of the micro and mesopores) and increased mass transport (due to the presence of large mesopores and macropores). Particularly, hierarchically porous metallosilicates have garnered much attention due to their multiple functionalities: catalysts, adsorbents or supports.

The main limitation of the hierarchical porous materials synthesized via the techniques reported to date in the scientific literature is that they are usually obtained in the form of powder that is difficult to be separarated from the reaction mixture, requiring high speed centrifugation or special filtration.

The aim of this work is to report an easy method for the synthesis of the porous zirconium silicates in the form of macrospheres with good mechanical, thermal and chemical stability, which can be easily separated and recovered by simple filtration. The metallosilicate macrospheres were obtained by the spray gelling technique, using the multi templating method. Tetraethyl orthosilicate was used as silica source. The chitosan played a dual role (structure and shape generating agent), while other inexpensive and easily accessible biomaterials such as yeast, gelatin and sugar were used as pore generators. The synthesized macrospheres were used as adsorbent for the removal of the Basic Blue 3 cationic dye from aqueous solutions.

2. Experimental

2.1. Reagents and materials

$ZrOCl_2 \cdot 8H_2O$, ammonia solution (25%), tetraethylorthosilicate, HCl solution (37%), chitosan with high molecular weight and agar were purchased from Aldrich. Commercial yeast, sugar and gelatin were used into the experiments. The chitosan solution was prepared by dissolving of 4g of chitosan in 96 mL acetic acid solution (92 mL distilled water and 4 mL acetic acid 98%). Commercial basic dye Astrazon Blue BG (C.I. Basic Blue 3) used as adsorbate was obtained from Dye Star Company and was used without any further purification.

2.2. Synthesis of the metallosilicate macrospheres

The zirconium silicate macrospheres were prepared as follows:

(1) Obtaining of the *solution A*: 3 mL of TEOS were poured into a solution containing 11 mL of water, 0.45 mL of HCl 37% and 0.72 g $ZrOCl_2 \cdot 8H_2O$ and the mixture was magnetically stirred for 6 hours at the room temperature.

(2) Preparation of the *templating mixture B*: 2.7 g of yeast were dispersed in 17 ml of distilled water and the suspension was heated at 85ºC for 1.5 hours. 0.36 g of agar, 0.60 g sugar and 0.36 g of gelatine were then added and the stirring continued for 1 hour at the same temperature. The mixture was cooled up to the room temperature and 0.45 mL HCl 37% solution were added and the stirring continued for 15 minutes. Finally, 9 g of 4% chitosan solution were introduced and the resulted gel was mixed for 1 hour.

(3) Homogenization under stirring for 2 hours of the gel resulted by pouring of the solution A over the mixture B.

(4) Dropping of the gel in 25% ammonia solution and keeping of the obtained macrospheres into this solution for 20 minute to harden.

(5) Separation of the hybrid inorganic-organic composite macrospheres by filtration, followed by drying (at 60ºC for 8 hours and subsequently at 160ºC for 12 hours).

(6) Calcination at 625ºC for 12 hours in order to obtain the porous structure by the removal of the organic templating mixture.

2.3. Physicochemical characterization

The FTIR spectra were recorded on a Nexus 470 FTIR spectrometer using the KBr-disk technique. The registrations performed in the wavenumber range $4000 \div 400$ cm^{-1} were obtained by the co-addition of 32 scans with a resolution of 2 cm^{-1}. The wide angle X-ray diffraction pattern of the sample was recorded on a Philips XPERT MPD diffractometer in the 2θ range of $10^o \div 70^o$, at a scanning speed of 1º/min, using a nickel-filtered Cu K_α radiation ($\lambda = 0.15418$ nm). SEM micrographs and EDX spectra were obtained with an FEI Quanta 200 Scanning Electron Microscope equipped with an EDAX Genesis 400 with Si(Li) detector, type Sapphire. The measurements were carried out at an accelerating voltage of 20 kV, with a Large Field Detector (LFD) in the low Vacuum Mode.

The nitrogen adsorption isotherm was measured at liquid nitrogen temperature (77 K) using a Nova 2200e system (Quantachrome).

2.4. Adsorption studies

The zirconium silicate beads were tested as adsorbent for the removal of the Astrazon Blue BG dye from aqueous solutions. The adsorption experiments were carried out at different initial dye concentrations and various adsorbent concentrations. In all the experiments the temperature was kept at 22°C and the stirring speed was 250 rpm. The unknown dye concentrations from the residual solutions were determined from the calibration curve by using a UV-Vis spectrophotometer.

The percent removal of the dye (R%) and the equilibrium adsorption capacity q_e (mg/g) were calculated using Eqs.1 and 2:

$$R(\%) = \frac{c_0 - c_e}{c_0} \cdot 100 \quad (1)$$

$$q_e = \frac{(c_0 - c_e) \cdot V}{w} \quad (2)$$

where c_0 (mg/L) and c_e (mg/L) are the initial and respectively the equilibrium dye concentrations in the liquid-phase, V (L) is the volume of the solution and m (g) is the amount of adsorbent.

2.5. Error analysis

The best fit kinetic/adsorption model was selected based on the linear regression correlation coefficient values R^2, and the average percentage error (APE). The average percentage error (APE) was calculated using the following equation:

$$APE(\%) = \frac{\sum_{i=1}^{n} \left| (q_{exp} - q_{calc})/q_{exp} \right|}{n} \cdot 100$$

where, q_{exp} (mg/g) is the experimental adsorbed amount, q_{cal} (mg/g) is the theoretical adsorbed amount and n is the number of experimental data.

3. Results and discussions

The synthesized macrospheres used for the adsorption of the cationic dye from aqueous solutions have diameters comprised in the range 1.5 – 1.6 mm. Due to their size and strength the zirconium silicate spherical beads can be easily handled and recovered from the wastewaters.

3.1. Characterization of the zirconium silicate macrospheres

3.1.1. Energy dispersive X-ray analysis (EDX)

The elemental composition of the zirconium silicate macrospheres was determined by EDX analysis (Fig. 1). The value of the Si/Zr mole ratio (Si: Zr = 1 : 0.162) for the calcined and washed sample is close to the value of the Si/Zr mole ratio (Si: Zr = 1 : 0.17) from the synthesis gel which confirms the efficient incorporation of the metal.

3.1.2. Wide angle X-ray diffraction analysis (WAXD)

The structural characterization by wide angle X-ray diffraction analysis was carried out in order to investigate the amorphous/crystalline structure of the sample. The diffractogram (Fig. 2) contains a single wide peak located between 2θ = 10º ÷ 30º, which indicates that the sample contain a high amount of amorphous zirconium silicate.

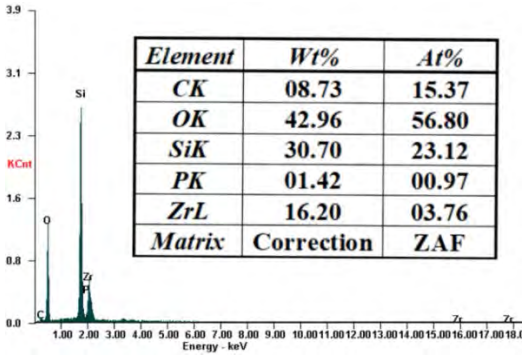

Fig. 1. EDX analysis of the zirconium silicate macrospheres

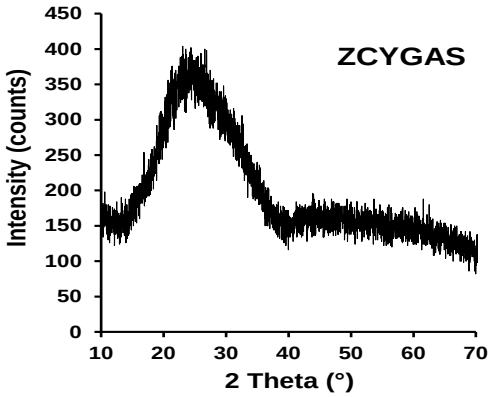

Fig. 2. X-ray diffraction spectrum of the synthesized zirconium silicate

The presence of this wide band and the pronounced background noise recorded during the whole XRD pattern suggests also the existence of some small size particles within the structure of the macrospheres. The absence of the peaks characteristic to zirconium oxide indicates the efficient incorporation of the zirconium into the silica network (or at most the presence of some small size oxide crystallites which are uniformly dispersed on the sample surface and cannot be put into evidence by XRD analysis).

3.1.3. Fourier transformed infrared spectrometry (FTIR)

FTIR analysis (Fig. 3) was performed in order to prove the formation of the Si-O-Zr bonds (incorporation of zirconium within the silica framework) and the Si-O-Si bonds. The spectral data of the zirconium silicate sample and the assignment of the absorption bands to their corresponding types of infrared vibrations are shown in Table 1.

Table 1. FTIR spectral data of the zirconium silicate sample

Peak position (cm^{-1})	***Assignment of the absorption bands***
460	overlap of the rocking bending mode vibrations of the Si-O and Zr-O bonds belonging to the Si-O-Si and Si-O-Fe linkages
801	overlap of the symmetric stretching vibrations of the O-Si-O and O-Zr-O bonds within the polyhedrons
1074	overlap of the asymmetric stretching mode vibrations of the O-Si-O and O-Zr-O bonds within the polyhedrons
1635	bending mode vibrations of the adsorbed water molecules
3461	stretching mode vibrations of the bridging OH groups

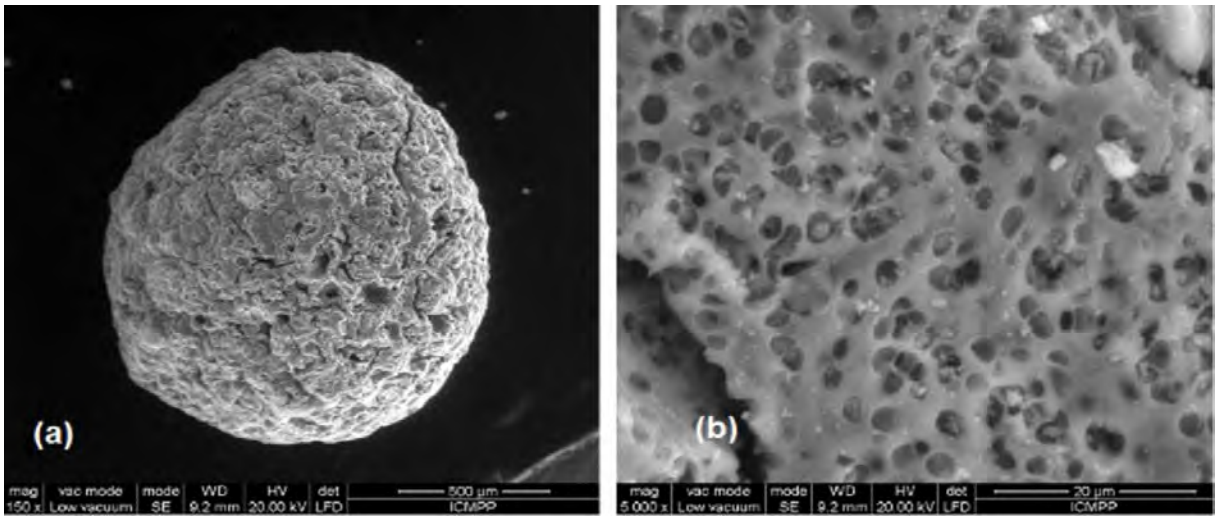

Fig. 4. SEM images of the zirconium silicate macrospheres:
(a) whole spherical bead; (b) detailed surface image

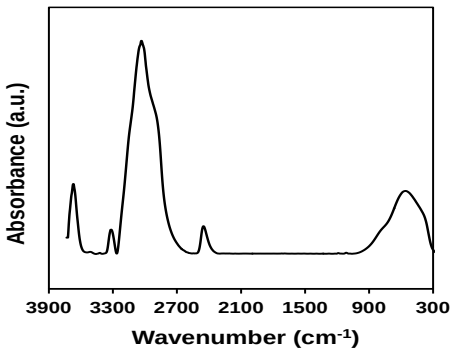

Fig. 3. FTIR spectrum of the zirconium silicate sample

The peaks that occur at 460 cm^{-1}, 801 cm^{-1} and respectively 1074 cm^{-1} prove the incorporation of the zirconium within the silica framework. The absence of the bands at 3757 cm^{-1} and 3780 cm^{-1} attributed to the terminal silanol groups and respectively to the Zr-OH groups show the effectiveness of the condensation reaction and the successful incorporation of the zirconium within the silica matrix (Mureșan et al., 2014, 2015, 2016).

3.1.4. Scanning electron microscope (SEM)

The surface morphology and the pore size of the zirconium silicate macrospheres were investigated by scanning electron microscopy (Fig. 4).

The low magnitude 150x electron microphotograph (Fig. 4a) shows that the zirconium silicate macrospheres look like it would be composed of „aggregates shaped like cereal flakes" and present some cracks in the form of slits on their surface. From the high magnitude 5000x electron microphotograph (Fig. 5b) it is noticed that the sample has a large number of the microns order sized pores which are relatively evenly distributed on its surface.

3.1.5. Determination of the textural properties from the nitrogen physisorption data

The nitrogen sorption experiments were performed in order to determine the textural properties of the synthesized samples. The recorded adsorption-desorption isotherm do not fit very well in the classification given by IUPAC (Fig. 5).

The adsorption branch is similar to the I(b) type isotherm up to the p/p^0 = 0.72 value of the relative pressure and looks like the type II isotherm for higher relative pressures (does not reach the final saturation plateau at high values of the relative pressure). The hysteresis loop is a hybrid between H_3 and H_4 types. It resembles better to the H_4 type hysteresis loop which is encountered in the case of the materials containing both micropores and mesopores, but also exhibit some features corresponding to the H_3 type hysteresis loop due to the presence of the large mesopores and macropores (Thommes et al., 2015). The pore size

distribution was determined from the adsorption branch of the isotherm using the Barret-Joyner-Halenda (BJH) model. The micropore volume V_μ = 0.053 (cc/g), mesopore volume V_m = 0.099 (cc/g), micropore surface area S_μ = 138.67 (m^2/g) and the external surface area S_{ext} = 132.27 (m^2/g) were calculated using the t-plot method. The BET surface area S_{BET} = 271 (m^2/g) was determined using the adsorption data from the relative pressure range comprised between $p/p^0 = 0.05 \div 0.35$.

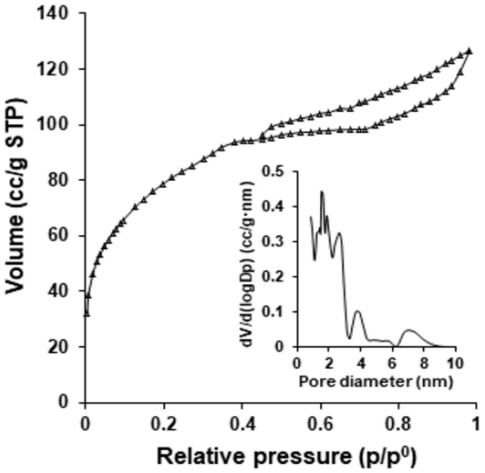

Fig. 5. Nitrogen adsorption-desorption isotherm and the pore size distribution

3.2. Adsorption studies

3.2.1. Effect of the initial dye concentration and contact time

The effect of the initial dye concentration (in the range from 60 to 150 mg/L) and of the contact time on the adsorption capacity of the zirconium silicate beads was investigated (Fig 6).

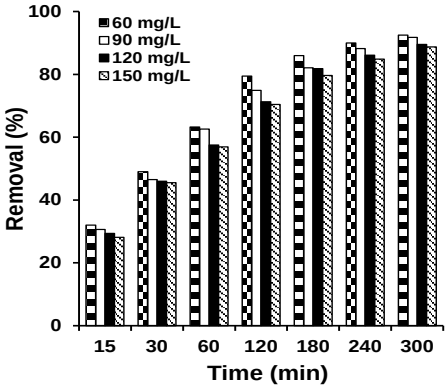

Fig 6. The effect of the initial dye concentration and of the time on the percentage of dye removed from the solution (adsorbent dosage 5 g/L, temperature 295 K, agitation speed 250 rpm)

The adsorption rate of the dye on the zirconium silicate beads is high in the first 60 min due to the availability of a high number of vacant sites. Thereafter, the adsorbed amount increases slowly by the prolonging of the contact time because of the repulsive forces that exhibit between the adsorbed molecules and the ones that exist in the liquid phase. The percentages of dye removed after 180 minutes were 85.9%, 82.1%, 81.8% and 79.6% and reached after 240 minutes at 90%, 88.2%, 86.1% and 84.8% for dye concentrations of 60 mg/L, 90 mg/L, 120 mg/L and 150 mg/L respectively. Given these results it would be advisable to work with dye concentrations between 90 - 120 mg/L and the adsorption time to be 240 minutes.

3.2.2. Effect of the adsorbent concentration on the dye removal

The adsorption capacity of the Astrazon Blue BG dye onto zirconium silicate macrospheres was studied for 2.5, 5, 7.5 and 10 g/L adsorbent dosages (Fig. 7).

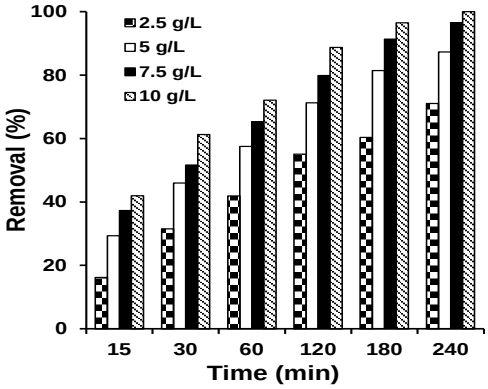

Fig 7. Effect of the adsorbent dosage on the percentage of dye removed from the solution (dye concentration 120 mg/L, temperature 295 K, stirring speed 250 rpm)

The results presented in Fig. 7 show that the percentage of the removed dye increases with the increase of the adsorbent concentration due to the increase of the number of the available adsorption sites.

3.2.3. Adsorption isotherms

Adsorption isotherms describe the relationship between the amount of dye adsorbed onto the adsorbent at equilibrium (q_e) and the equilibrium concentration of the dye remained in solution (C_e) at a given temperature. In order to quantify the affinity of the zirconium silicate macrospheres for the cationic dye the equilibrium adsorption data were analyzed using the Langmuir, Freundlich, Temkin and Dubinin-Radushkevich models (Abshirini et al., 2019; Ahmadi and Esmaeili., 2018; Abbasi et al., 2019; Esmaeili and Foroutan, 2019; Tamjidi and Esmaeili, 2019). The linear equations of the investigated adsorption isotherms are shown in Table 2. The calculated values of the parameters corresponding to the models of the studied adsorption isotherms are listed in the Table 3.

From the data presented in the Table 2 it can be deduced that the adsorption was better defined by the Temkin isotherm model (R^2 = 0.996) followed by the Dubinin-Radushkevich (R^2 = 0.986), Langmuir (R^2 = 0.982) and Freundlich (R^2 = 0.971) isotherm models.

Table 2. Isotherm models

Adsorption isotherm	*Linear equation*	*Plot*	*Slope*	*Intercept*
Langmuir	$\frac{C_e}{q_e} = \frac{1}{q_m} \cdot C_e + \frac{1}{K_L \cdot q_m}$	$\frac{C_e}{q_e}$ vs C_e	$\frac{1}{q_m}$	$\frac{1}{K_L \cdot q_m}$
q_m (mg/g) is the maximum amount of adsorbate per unit weight of adsorbent required to form a saturated monolayer of adsorbate molecules on the adsorbent surface; K_L (L/mg) is the Langmuir isotherm constant which is a measure of the affinity between adsorbate and adsorbent and is related to the free energy of adsorption. The Langmuir model assumes that the adsorption takes place onto homogeneous surfaces with a finite number of sites which have all the same activation energy (Langmuir, 1918).				
Freundlich	$logq_e = logK_F + \frac{1}{n} \cdot logC_e$	$logq_e$ vs $logC_e$	$\frac{1}{n}$	$logK_F$
K_F (mg/g) is a measure of the adsorption capacity (being related to the bonding energy) and 1/n corresponds to the strength of adsorption and to the surface heterogeneity. The value of n describes the adsorption characteristics as follows: if n = 1 the Freundlich expression reduces to a linear adsorption isotherm, which means a homogenous adsorption without interactions between the adsorbed species; n > 1, indicates that the adsorption is a favourable process; n < 1, indicates an unfavourable adsorption process (Freundlich, 1906).				
Temkin	$q_e = \frac{R \cdot T}{b_T} \cdot lnK_T + \frac{R \cdot T}{b_T} \cdot lnC_e$	q_e vs lnC_e	$\frac{R \cdot T}{b_T}$	$\frac{R \cdot T \cdot lnK_T}{b_T}$
b_T is the Temkin constant related to the heat of adsorption (J/mol) which indicates the adsorption intensity of the adsorbent; K_T (mg/L) is the Temkin constant related to the adsorption capacity. The Temkin isotherm assumes that the adsorption heat of the molecules decreases linearly with the surface coverage owing to a decrease of the adsorbent–adsorbate interactions during adsorption (Temkin and Pyzhev, 1940).				
***Dubinin-Radushkevich* (*D-R*)**	$lnq_e = lnq_D - B \cdot \varepsilon^2$	lnq_e vs ε^2	B	lnq_D
q_D is the theoretical saturation capacity (mg/g), B is a constant related to the mean free energy of adsorption per mole of adsorbate (mol^2/J^2); $\varepsilon = R \cdot T \cdot ln(1 + 1/C_e)$ is the Polanyi potential; $E = 1/\sqrt{2 \cdot B}$ is the mean sorption energy – based on this energy of activation one can predict whether the adsorption is physisorption or chemisorption. If the value of activation energy is in the range of 8 ÷ 16 kJ/mol is a physisorption process and if the value of activation energy is in the range of 20 ÷ 40 kJ/mol is a chemisorption process (Dubinin, 1960).				

Table 3. Isotherm constants for Astrazon Blue B adsorption onto zirconium silicate

Isotherm	*Parameters*		R^2	*APE*
Temkin	K_T	b	0.996	2.6
	0.507	199.53		
Dubinin-Radushkevich	q_D	B	0.986	3.63
	26.92	4 x 10^{-6}		
Langmuir	K_L	q_m	0.982	3.84
	0.04563	61.72		
Freundlich	K_F	n	0.971	5.12
	3.53	1.371		

The D-R mean adsorption energy E = 10 kJ/mol indicates an ionic exchange adsorption. The Freundlich constant n = 1.371 ($1/n$ = 0.729) indicates a favorable adsorption of the Astrazon Blue BG dye onto the zirconium silicate macrospheres.

3.2.4. Adsorption kinetics

The kinetics of the adsorption process was studied in order to provide data concerning the uptake rate of the Astrazon Blue BG dye and the mechanism of adsorption. Four kinetic models (Table 4) were selected and compared in order to find the best fitting model that to describe the sorption of the cationic dye onto the zirconium silicate macrospheres. The calculated values of the parameters corresponding to the adsorption kinetic models (pseudo first order model, pseudo-second order model, Elovich model and modified Freundlich model) are summarized in Table 5. For dye concentrations up to 90 mg/L the adsorption process proceeds fast, since the number of active centers located on the macrospheres surface and on the surface of pores with larger diameters is large enough to retain the dye molecules. For this reason, the adsorption process is better described by a second order kinetic model.

At higher concentrations of adsorbate (greater than 90 mg/L the adsorption process is better described by the Elovich model, which is more suitable for describe slow adsorption processes. Slower adsorption can be explained as follows: dye molecules must reach to the less accessible adsorption centers located in the narrower pores (adsorption times are higher due to the slow internal diffusion). The intraparticle diffusion kinetic model provides information about the mechanisms involved in the adsorption process**.**

The plot of q_t vs. $t^{0.5}$ for the adsorption of Astrazon Blue BG dye on the zirconium silicate beads (Fig. 8) show three linear sections: the first portion corresponds to the fast uptake of the dye molecules on the external surface area of the adsorbent beads; the

second straight portion is attributed to the gradual adsorption stage**;** the third linear portion is attributed to the final equilibrium stage indicating the saturation of the adsorbent surface. The occurrence of the several linear regions is due to the difference between the rate of the mass transfer from the initial stage and the rates of mass transfer that correspond to the other stages of the adsorption process.

3.6. Regeneration and reuse of the adsorbent

In order to investigate the efficency of the zirconium silicate beads, the synthesized macrospheres were reused 10 times. After each use the adsorbent was regenerated by calcination at 600°C for 2 hours to remove the adsorbed dye.

Table 4. Kinetic adsorption models

Kinetic model	Linear equation	Plots	Slope	Intercept
Pseudo first order	$\frac{1}{q_t} = \frac{k_1}{q_e} \cdot \frac{1}{t} + \frac{1}{q_e}$	$\frac{1}{q_t}$ vs $\frac{1}{t}$	$\frac{k_1}{q_e}$	$\frac{1}{q_e}$
k_1 is the pseudo first order rate constant of adsorption (min^{-1}); q_e and q_t (mg/g) are the amounts of adsorbed dye per unit mass of adsorbent at the equilibrium and respectively at time t (min); The model is commonly used for homogeneous sorbents and physical sorption and supposes that the rate of adsorption is influenced by the adsorbate concentration and by the number of free sites for adsorption (Lagergren and Svenska, 1898).				
Pseudo-second order	$\frac{t}{q_t} = \frac{1}{k_2 \cdot {q_e}^2} + \frac{1}{q_e} \cdot t$	$\frac{t}{q_t}$ vs t	$\frac{1}{q_e}$	$\frac{1}{k_2 \cdot {q_e}^2}$
k_2 is the pseudo second order rate constant of adsorption (g/mg·min); q_t and q_e (mg/g) are the amounts of dye adsorbed at time t and at equilibrium respectively; $k_2 \cdot q_e^2$ is the initial adsorption rate (mg/g·min). The pseudo second order model suggests that the adsorption depends both on the adsorbate concentration as well as on the adsorbent concentration. The rate-limiting step is the sorption and the intraparticle diffusion has no role in the mass transfer of the adsorption process (Ho and McKay, 1999).				
Elovich	$q_t = b \cdot ln(a/b) + b \cdot ln(t)$	q_t vs $ln(t)$	b	$b \cdot ln(a/b)$
a = initial adsorption rate (mg/g·min); b = desorption constant related to the extent of surface coverage and to the activation energy for chemisorption (mg/g); q_t = the amount of dye adsorbed at time t (mg/g). This model is usually used in chemisorption on heterogeneous materials and covers a wide range of slow adsorption processes (Elovich, 1962).				
Intra-particle diffusion model	$q_t = k_{id} \cdot t^{0.5} + C_i$	q_t vs $t^{0.5}$	k_{id}	C_i
k_{id} ($mg/g \cdot min^{0.5}$) is the rate constant of stage i (obtained from the slope of the straight-line q_t versus $t^{0.5}$), C_i is proportional with the thickness of the boundary layer. If the intraparticle diffusion is the sole rate-controlling step the plot of q_t vs $t^{0.5}$ is linear over the whole time range and passes through the origin; when the sorption process is controlled by more than one mechanism (the adsorption process proceeds in several steps) the plot of q_t vs $t^{0.5}$ will show multiple linear regions with different slopes (Weber and Morris, 1963).				

Table 5. Kinetic data for Astrazon Blue BG sorption

Kinetic models	***Dye concentration (mg/L)***			
	60	90	120	150
$q_{e,exp}$ (mg/g)	10,60	17.93	25.13	28.83
Pseudo-first order				
k_1 (g/mg·min)	32.416	58.714	28.019	25.066
$q_{e,calc}$ (mg/g)	11.09	21.83	24.04	26.46
R^2	0.972	0.981	0.994	0.99
APE	0.88	6.24	2.94	3.48
Pseudo-second order				
k_2 (g/mg·min)	0.00274	0.00117	0.00114	0.00104
$q_{e,calc}$ (mg/g)	11.14	19.41	25.38	28.41
R^2	0.999 0.996	0.998	0.999	0.998
APE	0.84	3.64	3.66	4.46
Elovich				
a (mg/g·min)	0.811	0.976	1.981	2.4322
b (mg/g)	2.224	4.116	4.844	5.297
$q_{e,calc}$ (mg/g)	11.985	20.409	26.656	29.763
R^2	0.985	0.979	0.997	0.999
APE	3.58	3.71	1.71	0.98
Intraparticle diffusion				
$k_{i,I}$ ($mg/g \cdot min^{0.5}$)	0.9306	1.528	2.1104	2.399
R^2	0.999	0.997	0.987	0.983
$k_{i,II}$ ($mg/g \cdot min^{0.5}$)	0.3391	0.5584	0.8889	0.9788
$C_{i,II}$	4.768	7.840	8.831	10.128
R^2	0.942	0.993	0.984	0.989
$k_{i,III}$ ($mg/g \cdot min^{0.5}$)	0.0918	0.1614	0.3237	0.423
$C_{i,III}$	8.4248	14.04	17.352	18.509
R^2	0.946	0.967	0.987	0.991

Table 6. Adsorption efficiency of different adsorbents for Basic Blue 3

Adsorbent	*Maximum adsorption capacity /Temperature*	*Reference*
Silica	11 mg/g (303 K)	Ahmad and Ram, 1992
CF clay	101 mg/g (298 K)	Bencheqroun et al., 2019
Sphagnum Magellanicum Peat	40.6 mg/g (303 K)	Contreras et al., 2007
Acrylic resin	59.53 mg/g (323 K)	Bârsănescu et al., 2009
Activated carbons from black sapote seeds	58–59.8 mg/g (303 K)	Peláez-Cid et al., 2019
Amberlite XAD-1180	35.7 mg/g (293 K)	Wawrzkiewicz, 2013
Pomelo Peel	23.87 mg/g (293 K)	Liew and Siew, 2014
Fe_3O_4	7.474 mg/g (298 K)	Muhammad et al., 2019
PANI (polyaniline)	8 mg/g (298 K)	Muhammad et al., 2019
PANI/Fe3O4	78.13 mg/g (298 K)	Muhammad et al., 2019
Zirconiumsilicate macrospheres	28.83 mg/g (295 K)	This study

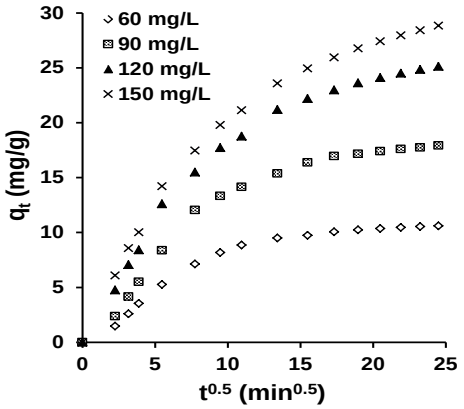

Fig. 8. The plot of the intraparticle diffusion model for adsorption of Astrazon Blue BG dye onto zirconium silicate macrospheres for different initial concentrations of adsorbate

No loss of the adsorptive capacity was noticed which represent an important avantage in view of potential industrial applications.

3.7. Comparison between the adsorption efficiency of different adsorbents for Basic Blue 3

A comparison between the maximum adsorption capacity of Basic Blue 3 dye on porous metallosilicate macrospheres and the maximum adsorption capacities of this dye on other adsorbents is presented in Table 6.

Although the values obtained on the zirconium silicate macrospheres are lower than some of the values previously reported for other adsorbents, the zirconium silicates used in this study have the great advantage that they can be easily separated and reused.

4. Conclusions

In this paper is presented an easy method for the preparation of porous zirconium silicate macrospheres by the spray gelling technique using the multi-templating method. Gelatine, agar, yeast, sugar and chitosan were used as pore generating agents. The multi templating technique allowed to obtain spherical form particles, with large pores, which facilitate the access of the reactants to the active centres located inside the micropores and the narrow mesopores. The wide angle X-ray diffraction, EDX and FTIR analyses proved the good incorporation of the zirconium within the silica framework. The zirconium silicate beads were used as adsorbents for the uptake of the Astrazon Blue BG cationic dye from aqueous solutions.

The adsorption process was found to be dependent on the initial dye concentration, adsorbent dose and contact time. Due to their dimensions (comprised between 1.5 mm and 1.6 mm) the macrospheres can be easily separated from the reaction mixture by simple filtration and reused several times.

Acknowledgements

This work was funded by the TUIASI research grant entitled „Macrospherical hierarchical porous metallosilicate materials obtained by mono or multi-templating technique: synthesis, characterization and application", project number 0199 / 2018, awarded by the "Gheorghe Asachi" Technical University from Iasi.

References

Abshirini Y., Foroutan R., Esmaeili H., (2019), Cr (VI) removal from aqueous solution using activated carbon prepared from *Ziziphus spina-christi* leaf, *Materials Research Express*, **6**, doi.org/10.1088/2053-1591/aafb45.

Ahmadi F., Esmaeili H., (2018), Chemically modified bentonite/Fe3O4 nanocomposite for Pb(II), Cd(II), and Ni(II) removal from synthetic wastewater, *Desalination and Water Treatment*, **110**, 154-167.

Abbasi S., Foroutan R., Esmaeili H., Esmaeilzadeh F., (2019), Preparation of activated carbon from worn tires for removal of Cu(II), Ni(II) and Co(II) ions from synthetic wastewater, *Desalination and Water Treatment*, **141**, 269-278.

Ahmad M.N., Ram R.N., (1992), Removal of basic dye from waste-water using silica as adsorbent, *Environmental Pollution*, **77**, 79-86.

Al-Degs Y., Khraisheh M.A.M., Allen S.J., Ahmad M.N.A., (2001), Sorption behavior of cationic and anionic dyes from aqueous solution on different types of activated carbons, *Separation Science and Technology*, **36**, 91-102.

Atun G., Hisarli G., Kurtoglu A. E., Ayar N., (2011), A comparison of basic dye adsorption onto zeolitic materials synthesized from fly ash, *Journal of Hazardous Materials*, **187**, 562–573.

Bârsănescu A., Buhăceanu R., Dulman V., (2009), Removal of Basic Blue 3 by sorption onto a weak acid acrylic resin, *Journal of Applied Science*, **113**, 607-614.

Bellú S., Sala L., González J., García S., Frascaroli M., Blanes P., García J., Peregrin J. S., Atria A., Ferrón J., Harada M., Cong C., Niwa Y., (2010), Thermodynamic and Dynamic of Chromium Biosorption by Pectic and Lignocellulocic Biowastes, *Journal of Water Resource and Protection*, **2**, 888-897.

Bencheqroun Z., El Mrabet I., Kachabi M., Nawdali M., Neves I., Zaitan H., (2019), Removal of basic dyes from aqueous solutions by adsorption onto Moroccan clay (Fez City), *Mediterranean Journal of Chemistry*, **8**, 158-167.

Betega de Paiva L., Francisco R. V. D., Ana Morales A., (2008), Organoclays: Properties, Preparation and Applications, *Applied Clay Science*, **42**, 8-24.

Brião G.V, Jahn S.L., Foletto E.L., Dotto G.L., (2018), Highly efficient and reusable mesoporous zeolite synthetized from a biopolymer for cationic dyes adsorption, *Colloids and Surfaces A: Physicochemical and Engineering Aspects*, **556**, 43-50.

Chih-Hung H., Chang K.P., Hong D.O., Chiang Y.C., Wang C.F., (2011), Adsorption of cationic dyes onto mesoporous silica, *Microporous and Mesoporous Materials*, **141**, 102-109.

Contreras E., Martinez B., Sepúlveda L., Palma C., (2007), Kinetics of basic dye adsorption onto *Sphagnum magellanicum* Peat**,** *Adsorption Science & Technology*, **25**, 637-646.

Cristiana R., Ionica I., Moater E. I., Stihi C., (2009), Decolourization of textile wastewater containing green cationic dye by AOPs, *Ovidius University Annals of Chemistry*, **20**, 66-71.

Dubinin M. M., (1960), The potential theory of adsorption of gases and vapors for adsorbents with energetically non-uniform surface, *Chemical Reviews*, **60**, 235-266.

Elovich S.Y., Larionov O.G., (1962), Theory of adsorption from solutions of non-electrolytes on solid (I) equation adsorption from solutions and the analysis of its simplest form, (II) verification of the equation of adsorption isotherm from solutions, *Izvestiya Akademii Nauk SSSR, Otdelenie Khimicheskikh Nauk,* **2**, 209-216.

Esmaeili H., Foroutan R., (2019), Adsorptive behavior of methylene blue onto sawdust of sour lemon, date palm, and eucalyptus as agricultural wastes, *Journal of Dispersion Science and Technology*, **40**, 990-999.

Forgacs E., Cserhati T., Oros G, (2004), Removal of synthetic dyes from wastewaters: a review, *Environment International*, **30**, 953–971.

Freundlich H., (1906), Over the Adsorption in Solution, *The Journal of Chemical Physics*, **57**, 385-471.

Gottipati R., Mishra S., (2010), Application of biowaste (waste generated in biodiesel plant) as an adsorbent for the removal of hazardous dye – methylene blue – from aqueous phase, *Brazilian Journal of Chemical Engineering*, **27**, 357-367.

Gurses A., Hassani A., Kıransan M., Acıslı O., Karaca S., (2014), Removal of methylene blue from aqueous solution using by untreated lignite as potential low-cost adsorbent: Kinetic, thermodynamic and equilibrium approach, *Journal of Water Process Engineering*, **2**, 10-21.

Hammed A.K., Dewayanto N., Du D., Abrahim M.H, Nordin M.R., (2016), Novel modified ZSM-5 as an efficient adsorbent for methylene blue removal, *Journal of Environmental Chemical Engineering*, **4**, 2607-2616.

Ho Y.S., McKay G., (1999), Pseudo-second order model for adsorption processes, *Process Biochemistry*, **34**, 451-465.

Huang Z., Li Y., Chen W., Shi J., Zhang N., Wang X., Li Z., Gao L., Zhang Y., (2017), Modified bentonite adsorption of organic pollutants of dye wastewater, *Materials Chemistry and Physics*, **202**, 266-276.

Jamwal H.S., Kumari S., Chauhan G.S., Reddy N.S., Ahn J.H., (2017), Silica-polymer hybrid materials as methylene blue adsorbents, *Journal of Environmental Chemical Engineering*, **5**, 103-113.

Junxing H., Ji L., Li C., Hu C., Wu K., (2018), Show more Rapid, efficient and economic removal of organic dyes and heavy metals from wastewater by zinc-induced in-situ reduction and precipitation of graphene oxide, *Journal of the Taiwan Institute of Chemical Engineers*, **88**, 137-145.

Konicki W., Aleksandrzak M., Mijowska E., (2017), Equilibrium, kinetic and thermodynamic studies on adsorption of cationic dyes from aqueous solutions using graphene oxide, *Chemical Engineering Research and Design*, **123**, 45-49.

Kumar P.S., Ramalingam S., Sathishkumar K., (2011), Removal of methylene blue dye from aqueous solution by activated carbon prepared from cashew nut shell as a new low-cost adsorbent, *Korean Journal of Chemical Engineering*, **28**, 149-155.

Lagergren S., Svenska B. K., (1898), About the theory of so-called adsorption of soluble substance, *Kungliga Svensca Vetenskapsakad. Handling*, **24**, 1-35.

Langmuir I., (1918), The Adsorption of Gases on Plane Surfaces of Glass, Mica and Platinum, *Journal of the American Chemical Society*, **40**, 1361-1403.

Largitte L., Pasquier R., (2016), A review of the kinetics adsorption models and their application to the adsorption of lead by an activated carbon, *Chemical Engineering Research and Design*, **109**, 495-504.

Liew S.W., Siew T.O., (2014), Removal of Basic Blue 3 dye using pomelo peel, *Asian Journal of Chemistry*, **26**, 3808-3814.

Muhammad A., Anwar-ul-Haq A. S., Bilal S., Rahman G., (2019), Basic Blue dye adsorption from water using polyaniline/magnetite (Fe_3O_4) composites: kinetic and thermodynamic aspects, *Materials*, **12**, 1764.

Mureșan E.I., Cimpoeșu N., Bargan A., Istrate B., (2015), Effect of the template on the textural properties of the macrospherical trimodal metallosilicate materials, *Journal of Inorganic and Organometallic Polymers*, **25**, 1060-1068.

Mureșan E.I., Drobota M., Bargan A., Dumitriu C.A.M., (2014), Hard porous chromium containing macrospheres as new catalysts for the esterification reaction of acetic acid with epichlorohydrin, *Central European Journal of Chemistry*, **12**, 528-536.

Muresan E.I., Puitel A., Pui A., Radu C. D., Tampu D., Cimpoesu N., Sandu I., (2016), Hierarchically bimodal porous metallosilicate catalysts for acetolysis of epichlorohydrin, *Revista de Chimie*, **67**, 659-664.

Nassar M.Y., Abdelrahman E.A., (2017), Hydrothermal tuning of the morphology and crystallite size of zeolite nanostructures for simultaneous adsorption and photocatalytic degradation of Methylene blue dye, *Journal of Molecular Liquids*, **242**, 364-374.

Peige Q., Yixin Y., Xiaoting Z., Jiahua N., Yang H., Shufang T., Jinhua Z., Minghua L., (2018), highly efficient, rapid, and simultaneous removal of cationic dyes from aqueous solution using monodispersed mesoporous silica nanoparticles as the adsorbent, *Nanomaterials*, **8**, 1-14.

Peláez-Cid A.A., Hernández V.R., Herrera-González A. M., Bautista-Hernández A., Coreño-Alonso O., (2019), Synthesis of activated carbons from black sapote seeds, characterization and application in the elimination of heavy metals and textile dye, *Chinese Journal of Chemical Engineering,* doi.org/10.1016/j.cjche.2019.04.021.

Rima J.Z., Egidija Z., Rima K., Algirdas Z., (2003), The role of anionic substances in removal of textile dyes from solutions using cationic flocculants, *Colloids and Surfaces A: Physicochemical and Engineering Aspects, Engineering Aspects*, **214**, 37-47.

Rutkowska M., Piwowarska Z., Micek E., Chmielarz L., (2015), Hierarchical Fe-, Cu- and Co-Beta zeolites obtained by mesotemplate-free method. Part I: Synthesis and catalytic activity in N_2O decomposition, *Microporous and Mesoporous Materials*, **209**, 54-65.

Sohrabnezhad S., Pourahmad A., (2010), Comparison absorption of new methylene blue dye in zeolite and nanocrystal, *Desalination*, **256**, 84-89.

Sun J., Li Y., Liu T., Du Q., Xia Y., Xia L., Wang Z., Wang K., Zhu H., Wu D., (2014), Equilibrium, kinetic and thermodynamic studies of cationic red X-GRL adsorption on graphene oxide, *Environmental Engineering and Management Journal*, **13**, 2551-2559.

Sizykh M.R., Batoeva A.A., Khandarkhayeva M.S., (2018), Removal of dyes from water by galvanocoagulation, *Environmental Engineering and Management Journal*, **17**, 27-34.

Tamjidi S., Esmaeili H., (2019), Chemically modified CaO/Fe3O4 nanocomposite by sodium dodecyl sulfate for Cr (III) removal from water, *Chemical Engineering & Technology*, **42**, 607-616.

Tehrani-Bagha A.R., Nikkar H., Mahmoodi N.M., Markazi M., Menger F.M., (2011), The sorption of cationic dyes onto kaolin: Kinetic, isotherm and thermodynamic studies, *Desalination*, **266**, 274-280.

Temkin M.I., (1941), Adsorption equilibrium and the kinetics of processes on non-homogeneous surfaces and in the interaction between adsorbed molecules, *Zhurnal fizicheskoi Khimii*, **15**, 296-332.

Temkin M.J., Pyzhev V., (1940), Recent modifications to Langmuir isotherms, *Acta Physicochimica USSR*, **12**, 217-225.

Thommes M., Kaneko K., Neimark A.V., Olivier J.P., Rodriguez-Reinoso F., Rougerol J., Sing K.S.W., (2015), Physisorption of gases, with special reference of surface area and pore size distribution (IUPAC Technical Report), *Pure and Applied Chemistry*, **87**, 1051-1069.

Wang C., Yin J., Wang R., Jiao T., Huang H., Zhou J., Zhang L., Peng Q., Facile preparation of self-assembled polydopamine-modified electrospun fibers for highly effective removal of organic dyes, *Nanomaterials*, **9**, 116-133.

Wawrzkiewicz M., (2013), Removal of C.I. Basic Blue 3 dye by sorption onto cation exchange resin, functionalized and non-functionalized polymeric sorbents from aqueous solutions and wastewaters, *Chemical Engineering Journal*, **217**, 414-425.

Weber W.J.Jr., Morris J.C., (1963), Kinetics of Adsorption of Carbon from Solution, *Journal of the Sanitary Engineering Division*, *American Society of Civil Engineering*, **89**, 31-60.

Weber W.J., Morris, J.C., (1963), Kinetics of adsorption on carbon from solution, *Journal of the Sanitary Engineering Division ASCE*, **89**, 31-60.

Xu H.Y., Wu L.C., Shi T.N., Liu W.C., Qi S.Y., (2014), Adsorption of acid fuchsin onto LTA-type zeolite derived from fly ash, *Science China Technological Sciences*, **57**, 1127-1134.

Yang Z, Asoh T.A., Uyama H., (2019), Removal of cationic or anionic dyes from water using ion exchange cellulose monoliths as adsorbents, *Bulletin of the Chemical Society of Japan*, **92**, 1453-1461.

Zonoozi M.H., Moghaddam M.R.A., Maknoon R., (2018), Treatment of an azo dye - containing wastewater in integrated anaerobic-aerobic membrane sequencing batch reactor (MSBR) at different hydraulic retention times (HRTS), *Environmental Engineering and Management Journal*, **17**, 2667-2676.